Journal of Power Sources 187 (2009) 112–122

Contents lists available at ScienceDirect

Journal of Power Sources

journal homepage: www.elsevier.com/locate/jpowsour

# Characterization of a direct methanol fuel cell using Hilbert curve fractal current collectors

Yean-Der Kuan[a,*], Jing-Yi Chang[b], Shi-Min Lee[c], Shah-Rong Lee[d]

[a] Department of Refrigeration, Air-Conditioning and Energy Engineering, National Chun-Yi University of Technology, NO 35, Lane 215, Section 1, Chung-Shan Road, Taiping City, 411 Taichung County, Taiwan
[b] Department of Mechanical and Electro-Mechanical Engineering, Tamkang University, Tamsui, 251 Taipei County, Taiwan
[c] Department of Aerospace Engineering, Tamkang University, Tamsui, 251 Taipei County, Taiwan
[d] Department of Mechanical Engineering, Technology and Science Institute of Northern Taiwan, Peitou, 112 Taipei, Taiwan

ARTICLE INFO

*Article history:*
Received 13 September 2008
Received in revised form 22 October 2008
Accepted 23 October 2008
Available online 6 November 2008

*Keywords:*
Fractal
Hilbert curve
Current collector
Direct methanol fuel cell
DMFC

ABSTRACT

The current collector or bi-polar plate is a key component in direct methanol fuel cells (DMFCs). Current collector geometric designs have significant influence on cell performance. This paper presents a continuous type fractal geometry using the Hilbert curve applied to current collector design in a direct methanol fuel cell. The Hilbert curve fractal geometry current collector is named HFCC (Hilbert curve fractal current collector). This research designs the current collector using a first, second and third order open carved HFCC shape. The cell performances of the different current collector geometries were measured and compared. Two important factors, the free open ratio and total perimeter length of the open carved design are discussed. The results show that both the larger free open ratio and longer carved open perimeter length present higher performance.



## 1. Introduction

The fuel cell has great potential as a new generation power source. It is an energy generator that directly converts chemical energy stored in the fuel into electrical energy through an electrochemical reaction. It has the main advantages of high efficiency, low emissions, simple mechanism, no moving parts, silent operation and flexible scaling between power and capacity [1]. Among the different types of fuel cells, the direct methanol fuel cell (DMFC) is prominently considered as a substitute power source in portable applications, such as mobile telephones, PDAs, notebooks, camcorders and so on [2]. Compared with other types of fuel cells, the DMFC has the advantages of near atmospheric temperature operating conditions, fast and easy refueling, handy liquid fuel storage, higher power density, low cost methanol and natural air applicable. In addition, a DMFC is able to convert methanol directly into electricity without using a bulk reformer to generate hydrogen. Therefore, a DMFC is ready for miniature compact designs [3].

A DMFC usually operates at near room temperature and adopts either vapor or liquid methanol solution as the fuel. The anode, cathode and reactions are shown as follows.

$$\text{anode}: \quad CH_3OH + H_2O \rightarrow 6e^- + 6H^+ + CO_2 \tag{1}$$

$$\text{cathode}: \quad \frac{3}{2}O_2 + 6e^- + 6H^+ \rightarrow 3H_2O \tag{2}$$

$$\text{overall}: \quad CH_3OH + \frac{3}{2}O_2 \rightarrow 2H_2O + CO_2 \tag{3}$$

The reactants at the anode side are methanol and water. The oxidation reaction at the anode side coverts the reactant into hydrogen protons, electrons and carbon dioxide. The hydrogen protons are transported from the anode to the cathode through a polymer electrolyte membrane. The electrons are conducted through an external circuit from the anode current collector to the cathode current collector. The reduction reaction at the cathode side forms protons, electrons, and oxygen to water [4].

In general, the fuel cell performance is characterized using the cell potential vs. current density polarization curve. The polarization curve reflects the fuel cell characterization at three distinct regions: the activation polarization at low current densities, the ohmic losses at intermediate current densities and concentration polarization at high current densities. The fuel cell polarization curve is determined by measuring from the open circuit potential and taking voltage or current measurements at prescribed potential or current intervals [5].

* Corresponding author. Tel.: +886 4 23924505x8256; fax: +886 4 23932758.
*E-mail address:* ydkuan@ncut.edu.tw (Y.-D. Kuan).

0378-7753/$ – see front matter © 2008 Elsevier B.V. All rights reserved.
doi:10.1016/j.jpowsour.2008.10.094

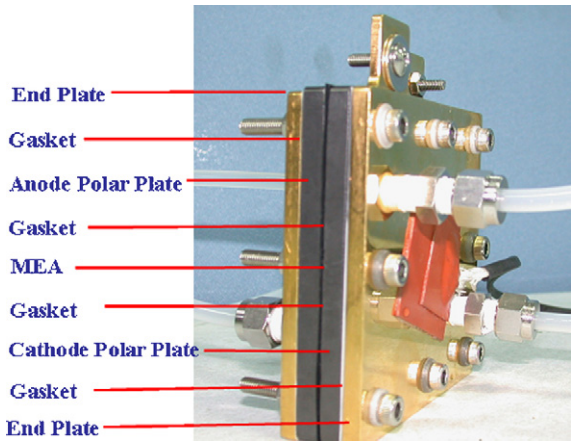


**Fig. 1.** A convectional single cell DMFC.

In a typical PEM/DMFC fuel cell, the bipolar plate has the important functions of carrying current away from the cell, distributing the fuel and oxidant within the cell, facilitating water and thermal management and separating individual cells in the stack. To maintain the fuel cell at high performance and stable operation, bipolar plate materials should have high electrical and thermal conductivity, good corrosion resistance, sufficient compressive strength and low density characteristics [6–8].

Conventionally, PEMFC/DMFC bipolar plates are stacked vertically with each bipolar plate serving as the anode for one cell and cathode in the next cell in multiple cells connected in series. Bipolar plates are made of graphite or metal. The flow channels inside the bipolar plates are grooved to distribute fuel and collect the electrical charge. For example, a convectional single cell DMFC is shown in Fig. 1, composed of an anode end plate, MEA, anode polar plate, cathode polar plate and one gasket placed between each pair of components to prevent liquid/gas leakage. The anode and cathode polar plates are made of graphite. The flow channel is grooved in the polar plate to distribute the fuel or gas as shown in Fig. 2. Each polar plate simultaneously serves as both a current collector and flow board. Experimental investigations of the anode flow effect on the convectional DMFC field design were conducted extensively.

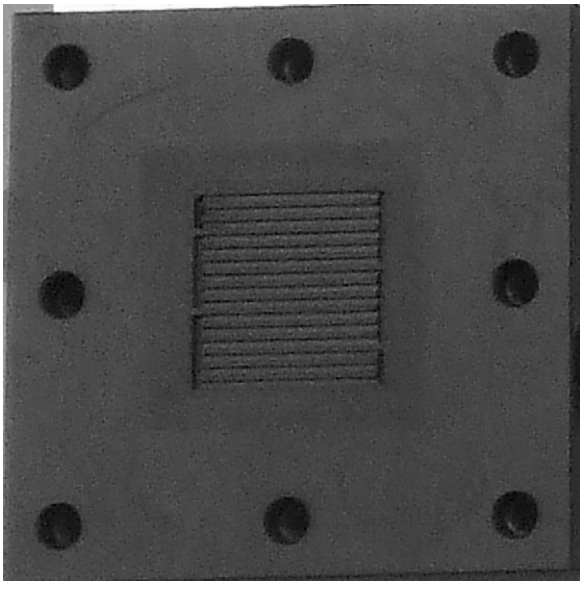

**Fig. 2.** A polar plate with the grooved flow channel.

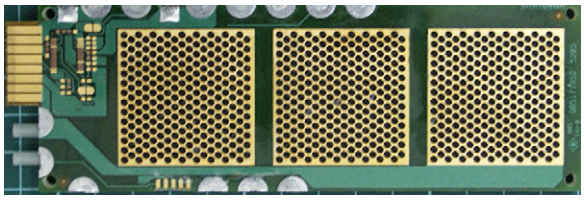

**Fig. 3.** A planar type PCB–DMFC module.

The bubble behavior could be observed using transparent enclosures. A DMFC with a single serpentine flow field (SSFF) exhibited better performance than the parallel flow fields (PFF) did. In a further study on the SSFF effect, Yang and Zhao found that an open ratio of around 50% led to the best cell performance at moderate and high methanol solution flow rates. They also indicated that a longer flow channel led to better performance but a larger pressure drop, which might cause more pumping power consumption by the fuel supply system [9]. PEMFC/DMFC planar interconnection designs have recently appeared as alternatives to vertical stacking. The cells are connected laterally rather than vertically. The planar series interconnection construction can yield better volumetric packaging compared to vertical stacks. This allows greater design flexibility for portable applications [5].

The printed circuit board (PCB) technology is a well-known low cost process and well established for mass production first applied to fuel cell fabrication by O'Hayre et al. and A. Schmitz et al. The PCB fabrication process is especially suitable for making the DMFC into a planar array [10–12]. Fig. 3 is an example of the planar type PCB–DMFC formed as a module with three cells. The construction of this PCB–DMFC is shown in Fig. 4. The components include the anode flow board, prepreg (PP), anode current collector, PP, MEA, PP, and cathode current collectors. There is no bipolar plate in this structure and the current collector and flow board are no longer combined. Instead, current collectors with openings to collect electrons and flow boards to distribute the fuel among the cells are used. More design considerations are needed for the planar PCB–DMFC module and module stack design. For example, the module with a single fuel inlet and single fuel outlet is preferred because this could simplify the fuel delivery tubes arrays and connections. The bubble choking at the anode and water blocking at the cathode are two issues that might degrade the DMFC performance. Therefore, it is important to deliver enough fuel and air through the cells in a module or modules in a stack [13].

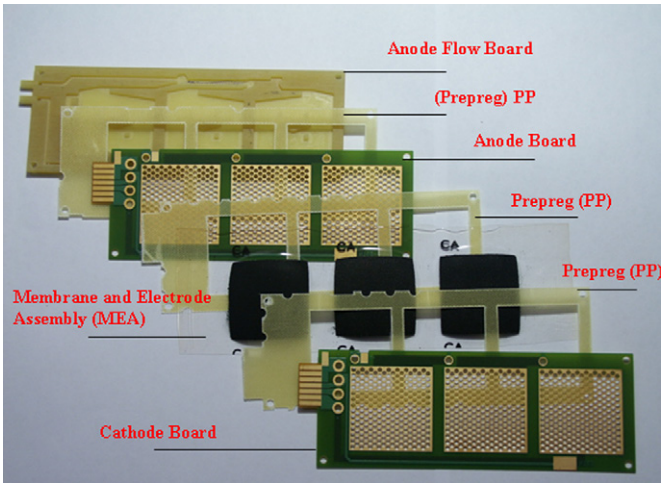


**Fig. 4.** The components of the PCB–DMFC.

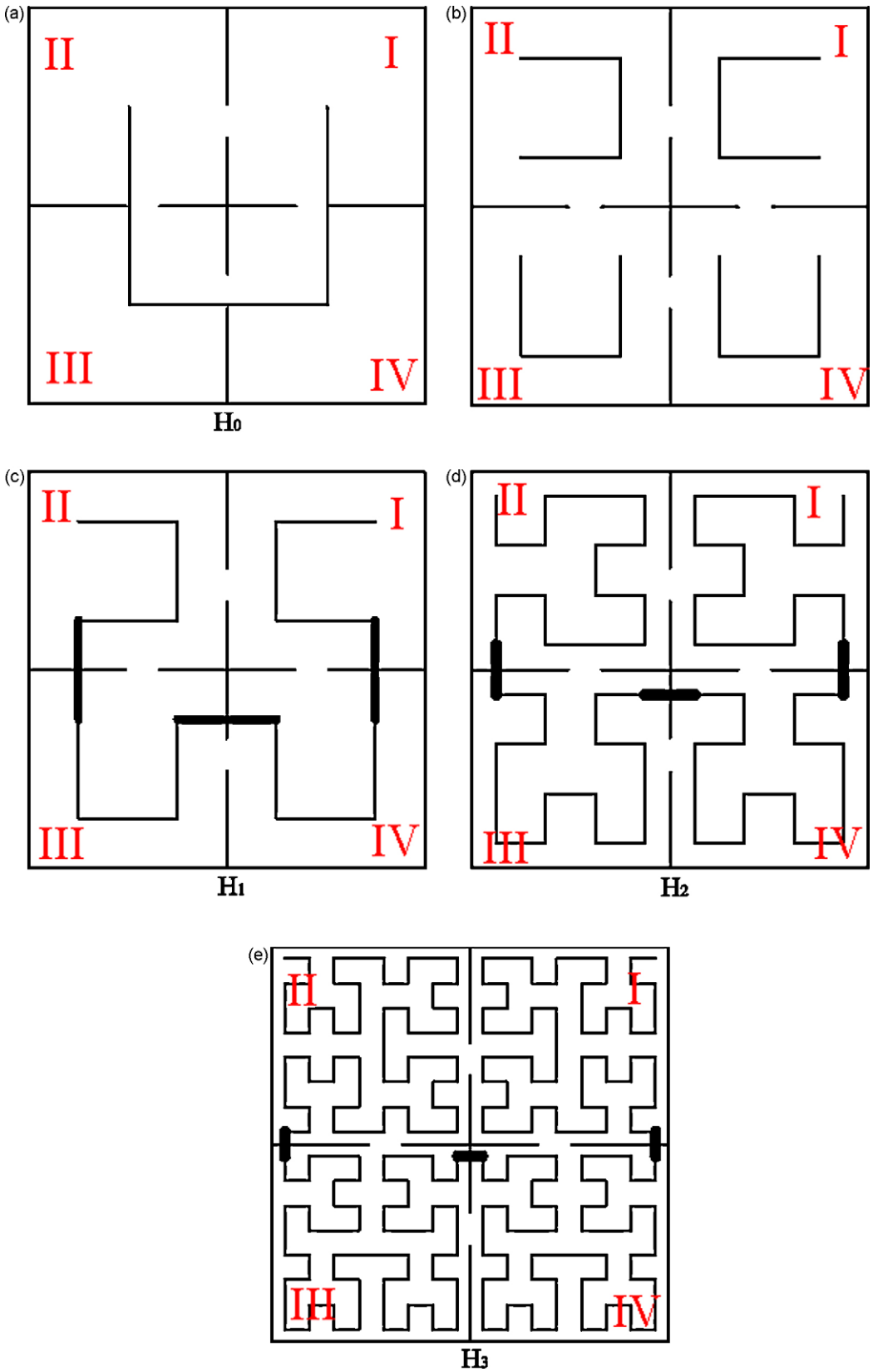


**Fig. 5.** Construction of the Hilbert curve fractal geometries, (a) 0th order Hilbert curve, (b) Four copies of the 0th order Hilbert curves (1/2 size), (c) 1st order Hilbert curve, (d) 2nd order Hilbert curve, (e) 3rd order Hilbert curve.

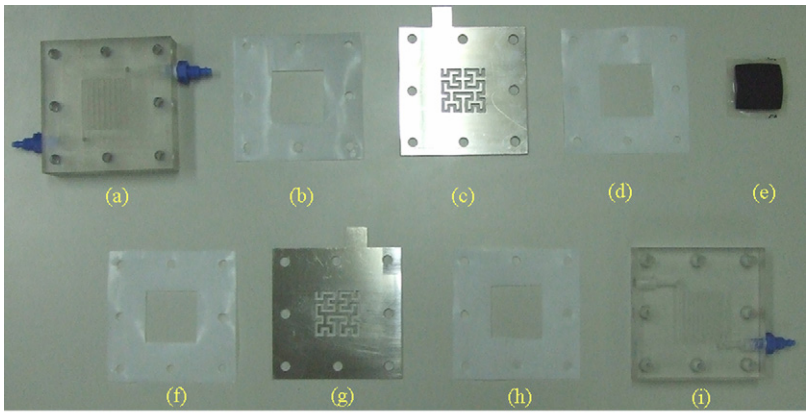


(a) Anode flow board, (b) Gasket, (c) Anode current collector, (d) Gasket, (e) MEA, (f) Gasket, (g) Cathode current collector, (h) Gasket and (i) Cathode airflow board.

**Fig. 6.** Single cell DMFC test fixture components, (a) anode flow board, (b) gasket, (c) anode current collector, (f) gasket, (e) MEA, (f) gasket, (g) cathode current collector, (h) gasket, and (i) cathode airflow board.

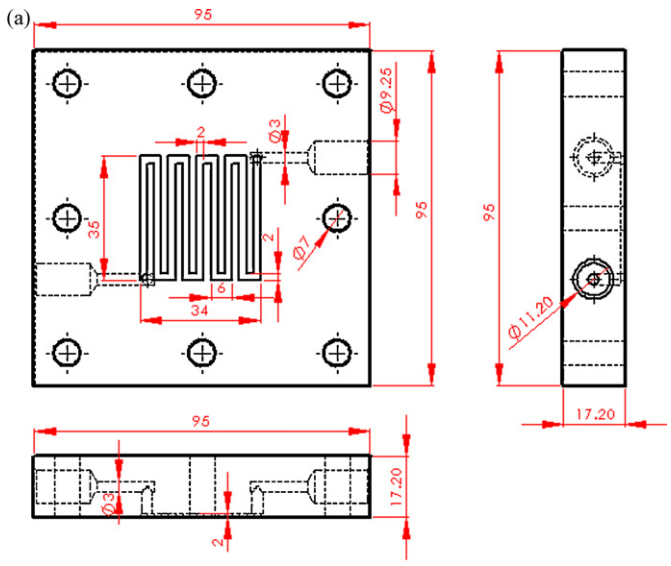


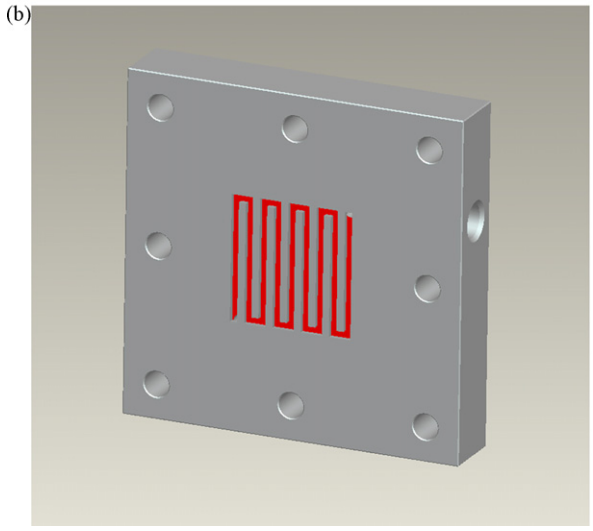


**Fig. 7.** The flow board (a) dimension of the flow board, (b) 3D solid drawing.

As the PCB–DMFC current collectors are thin metal films with openings, they are not designed to transport fuel or air. The current collector design is important in the printed circuit board type fuel cells. Making a better current opening design is valuable but a limited amount of literatures focused on current collector opening design. Huang et al. [14] studied the breathing hole size effect on a DMFC current collector via CFD simulation. Their CFD model did not include the anode reaction. Their simulation results showed that a larger breathing hole increases the ohmic resistance penalty and the area in contact with the fresh air reduces the concentration polarization. However, their numerical results were not compared with the experiments. Recently, Kuan and co-workers [15] made systematic experimental studies on the opening effects on the current collectors in DMFC performance. Their investigation was accomplished using a single cell DMFC in which the current collectors had Sierpinski carpet fractal holes. Two important factors could be involved: the open ratio and the total perimeter length of the holes. They found that a longer total hole perimeter length represented better cell performance, while a shorter total perimeter length and free open hole ratio lead to poor cell performance. The current collector with a longer total perimeter length under the same total free open ratio is recommended. In their study, following the rule of Sierpinski carpets, the total free open ratio of

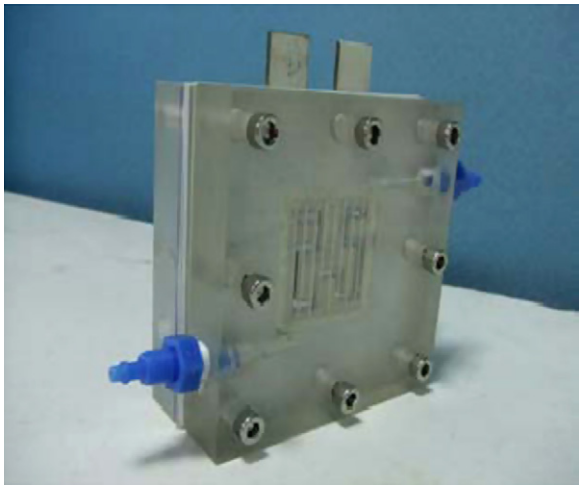

**Fig. 8.** The assembly of the single cell DMFC test fixture.

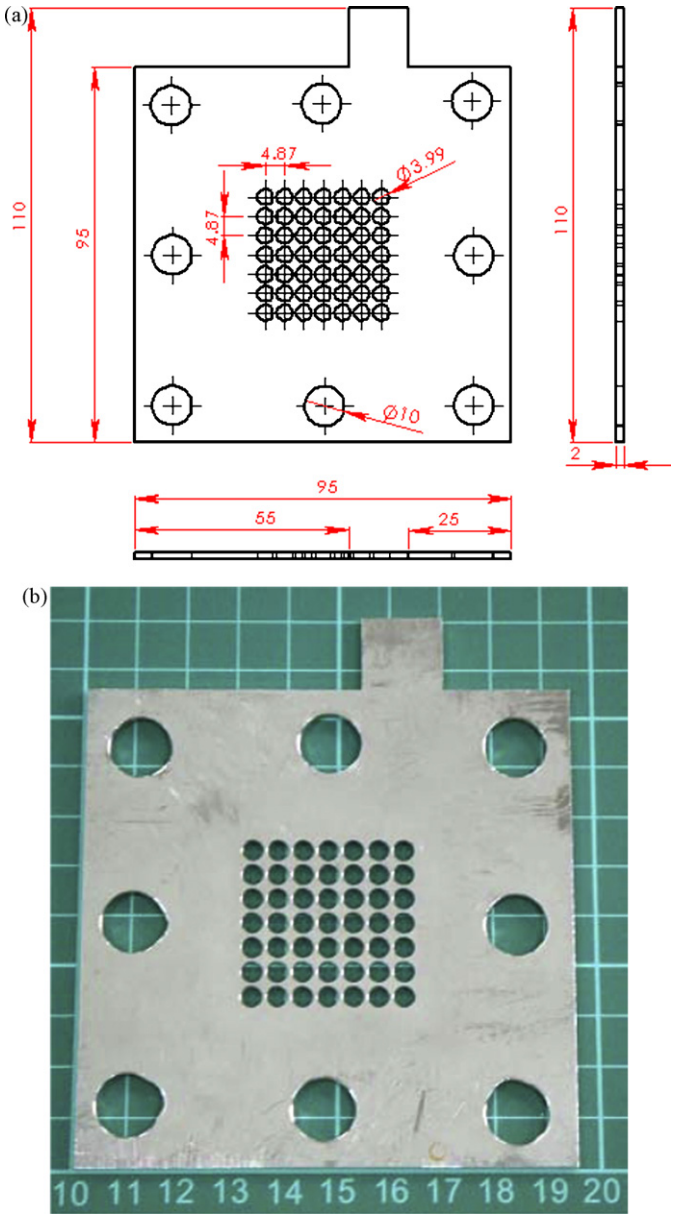


**Fig. 9.** Standard circular hole current collector (SCCC): (a) dimension of SCCC, (b) picture of SCCC.

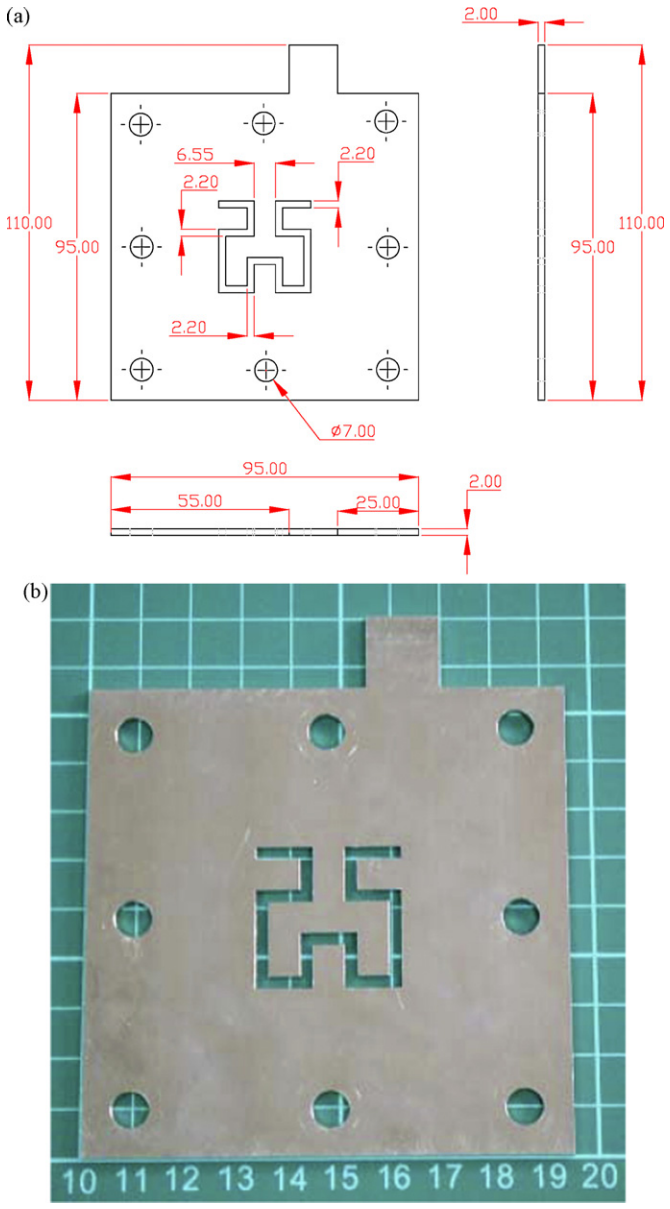


**Fig. 10.** 1st order Hilbert curve fractal current collector (HFCC1): (a) dimension of HFCC1, (b) picture of HFCC1.

the current collector was up to 30% and the total perimeter length for the openings was up to 503.96 mm under the 35 mm × 35 mm reaction area and 2nd order fractal. Therefore, further study on the current collector with larger total free open ratio and longer total opening perimeter length is desired. To increase the total free open ratio and longer total opening perimeter length the current collector is designed using a systematic space division method. The Hilbert curve, a continuous type fractal geometry and easy process at the current collector (single carved path), was adopted to design the current collectors and the total free open ratio, reaching up to 50%. The total opening perimeter length could be significantly increased.

## 2. Hilbert curve fractal generation rules

The fractal geometry is mathematically defined in "Haussdorff dimensions," a set of non-integers, with the theory proposed by Mandelbrot [16]. The fractal theory describes certain phenomena that are difficult to describe in very fine variations using conventional methods such as the contour of seashores, the slopes of valleys or patterns of clouds. The main characteristics of a fractal pattern are self-similarity, sub-divisibility and recursive nature. The fractal theory has been applied in many engineering fields such as the variations in entropy and heat transfer by Lee and Lin [17], tree networks for electronic cooling applications by Bejan et al. [18], circular heated surface cooling using fractal-like branching channel networks by Pence [19], fractal generation for heat sink fins by Lee et al. [20] and an automatic polishing path by Chen et al. [21].

The fractal theory was first applied to the fuel cell by Tuber et al. [22]. They presented fractal structures as PEMFC/DMFC flow fields for portable applications. They applied "FracTherm" theory to design fractal structures for a DMFC flow field on the bipolar plates. In their design, a multiple-branched structure with a smooth flow path, similar to biological fluid channels was presented. A performance comparison with serpentine and parallel flow fields was

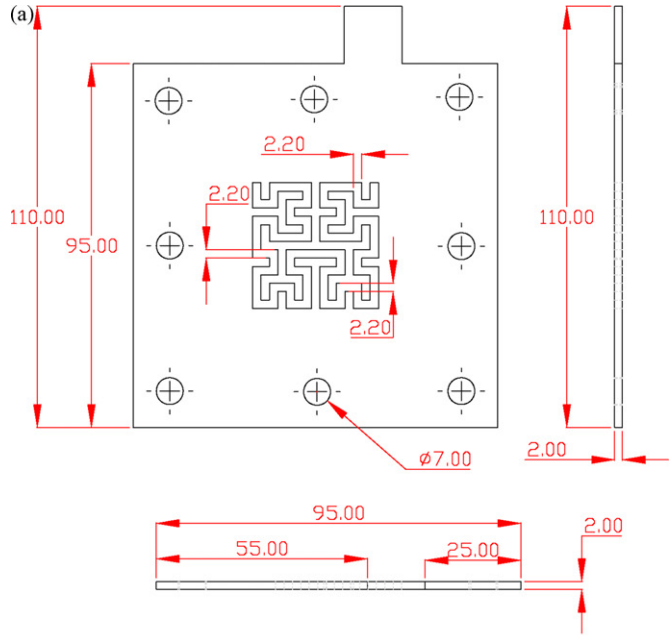


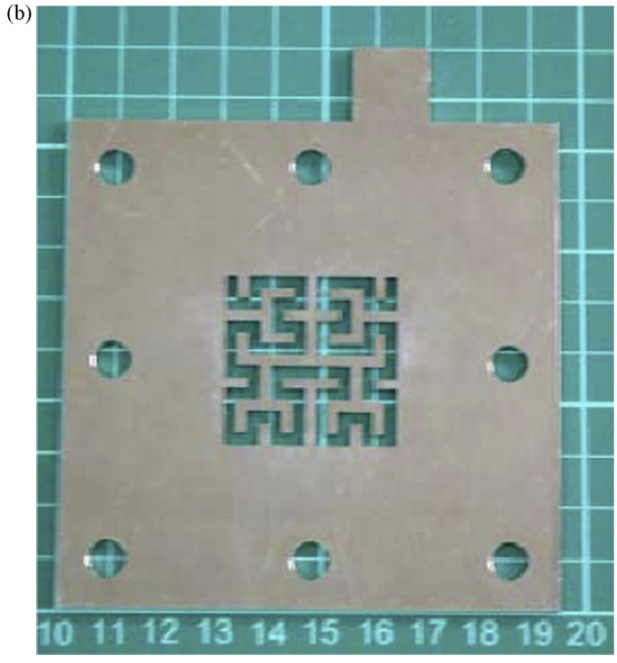


**Fig. 11.** 2nd order Hilbert curve fractal current collector (HFCC2): (a) dimension of HCCC2, (b) picture of HFCC2.

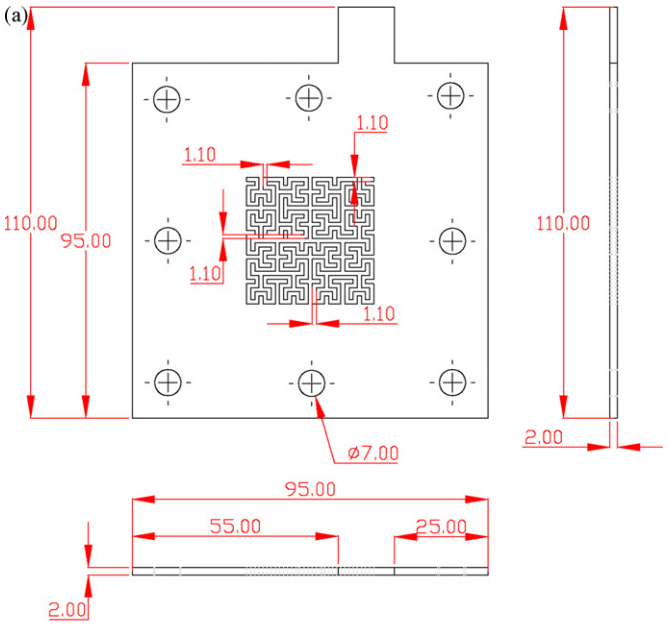


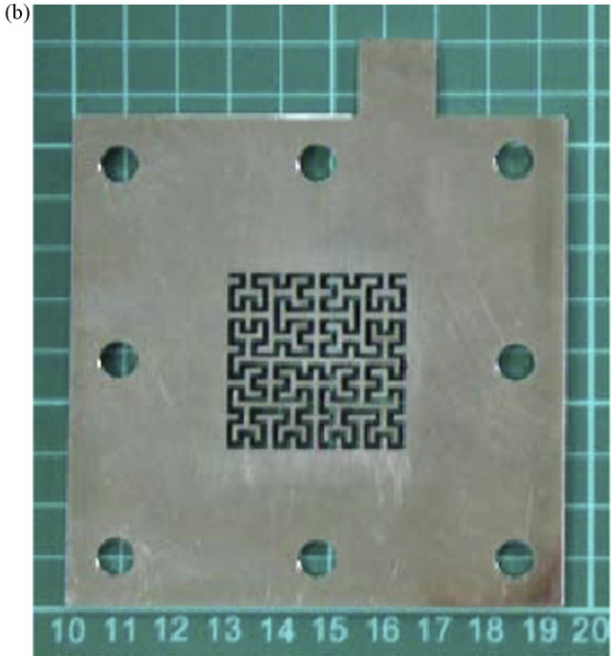


**Fig. 12.** 3rd order Hilbert curve fractal current collector (HFCC3): (a) dimension of HCCC3, (b) picture HFCC3.

made. The results showed that a serpentine flow channel yields better cell performance, but has much greater pressure drop across the channel. Both multiple-branched fractal and parallel flow fields create a lower pressure drop with similar performance. They also found that a lower pressure loss in the fractal flow field decreases the parasitic energy demand and achieves a more homogeneous flow distribution compared with a parallel design.

However, no further discussions on the fractal theory were applied to fuel cells in the literature, even though fractal theory

**Table 1**
Geometric information on current collectors.

| Geometry | | | | |
|---|---|---|---|---|
| Factors | Standard circular hole | 1st order Hilbert curve | 2nd order Hilbert curve | 3rd order Hilbert curve |
| Width of the Hilbert curve path (mm) | None | 2.20 | 2.20 | 1.10 |
| Total perimeter length of openings (mm) | 614.12 | 266.90 | 555.65 | 1117.82 |
| Total active MEA area (mm) | 1225 | 1225 | 1225 | 1225 |
| Total free open ratio (%) | 50.00 | 23.50 | 49.40 | 50.00 |

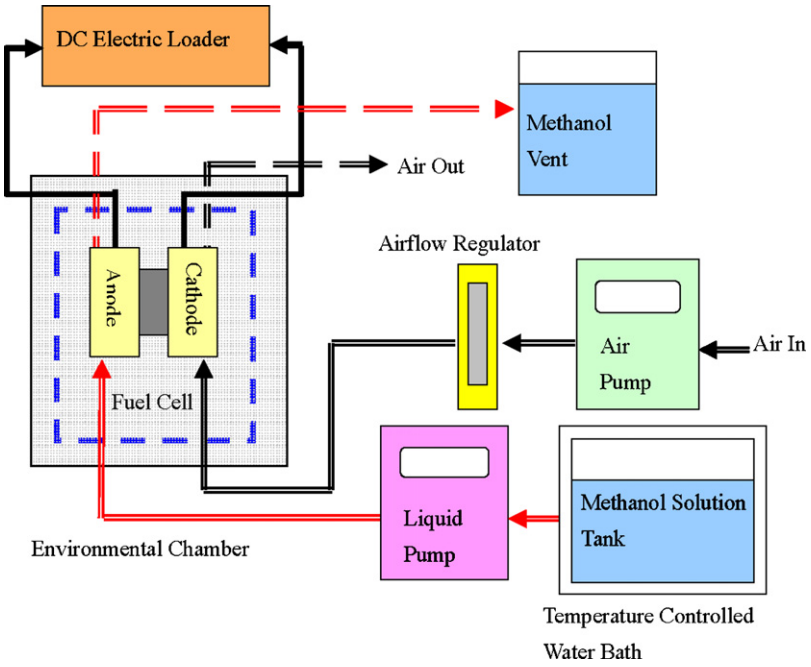


**Fig. 13.** Experimental setup.

generated systemic geometry in a previous work by Kuan and co-workers [15]. They proposed a type of current collector with Siepinski carpet fractal geometry [23,24]. Their current collector design included 1st and 2nd Siepinski carpet fractal hole arrangements and the standard holes arrangement. A series of experiments were conducted and found the total free open ratio and the perimeter length of the holes as two important factors. They concluded that a longer total holes perimeter represented better cell performance,

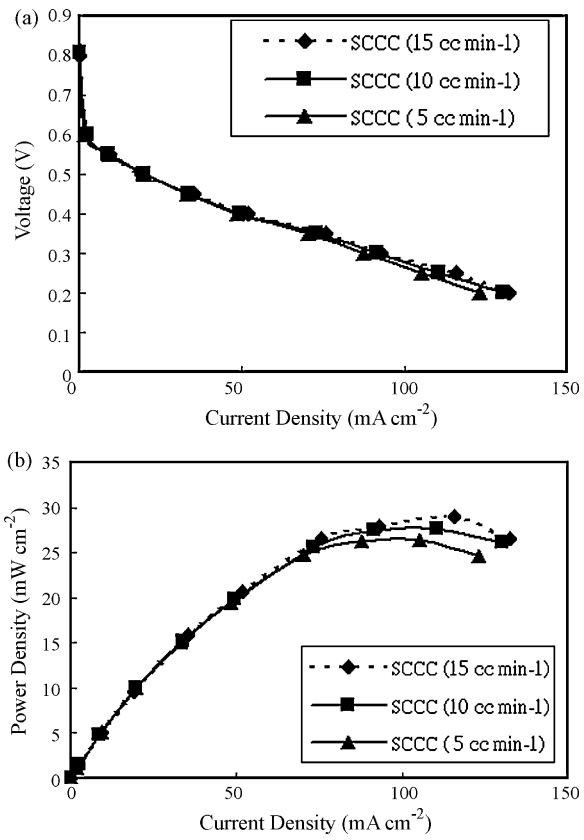


**Fig. 14.** Performance comparison of the DMFC with SCCC under different anode flow rate: (a) *I–V* curves, (b) *I–P* curves.

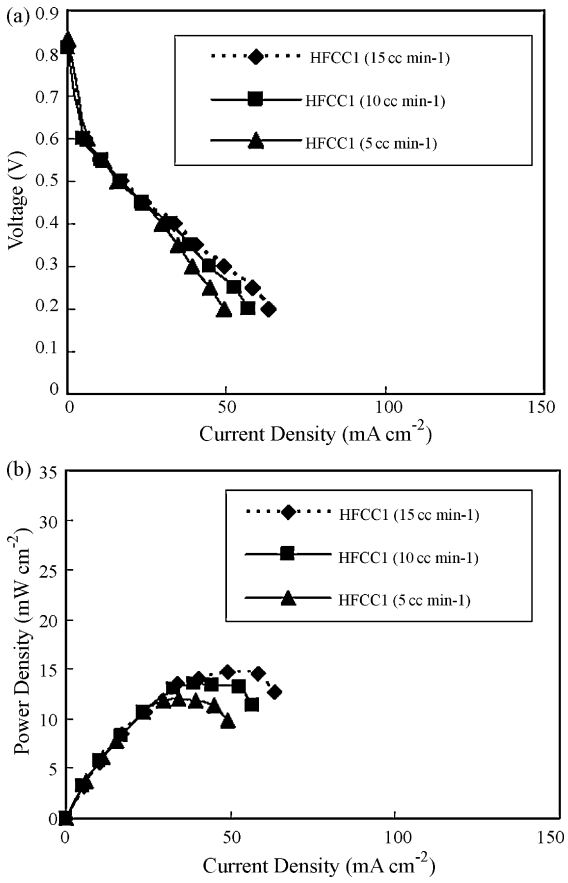


**Fig. 15.** Performance comparison of the DMFC with HFCC1 under different anode flow rate: (a) *I–V* curves, (b) *I–P* curves.

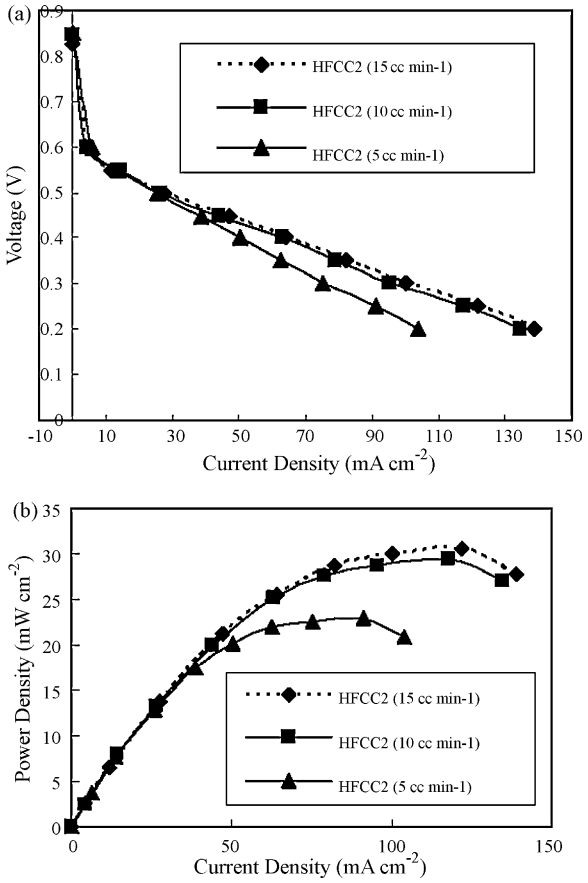


**Fig. 16.** Performance comparison of the DMFC with HFCC2 under different anode flow rate: (a) *I–V* curves, (b) *I–P* curves.

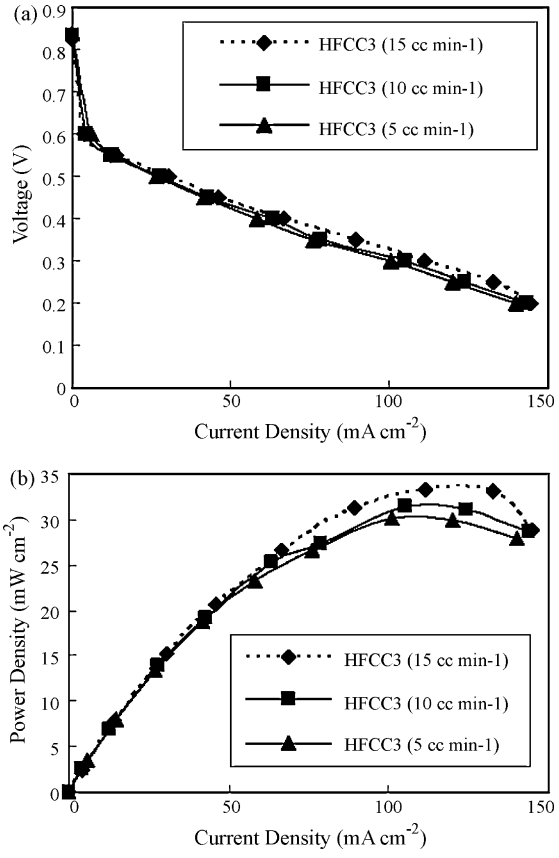


**Fig. 17.** Performance comparison of the DMFC with HFCC3 under different anode flow rate: (a) *I–V* curves, (b) *I–P* curves.

while a shorter total perimeter length and free open hole ratio lead to poor cell performance. A longer total perimeter length under the same total free open ratio is recommended.

The fractal geometry adopted in this research is the Hilbert curve, which was first described by Hilbert in 1891 [25]. The Hilbert curve is a continuous space filling curve that fills a square and is typically defined as the limit of a sequence of curves defined iteratively and that has only short vertical and horizontal jumps between the points in a square grid with a size of $2 \times 2$, $4 \times 4$, $8 \times 8$, $16 \times 16$ or any other power of 2. At all stages each curve has neither self-intersections nor touching points. The square area construction filled by a Hilbert curve is described as follows. First, divide the square into four quarters. The 0th order Hilbert curve $H_0$ connects the centers of the quadrants using three line segments, as shown in Fig. 5a. In the 1st order Hilbert curve construction step reduce 1/2 of $H_0$ produce four copies and place those four copies into the quarters. Next rotate the curve in the first quadrant clockwise and the curve in the second quadrant counterclockwise, as shown in Fig. 5b. Then connect the start and end points of these four curves using three line segments 1/2 size and the resulting curve is the first order Hilbert curve $H_1$, as shown in Fig. 5c. In the 2nd order Hilbert curve construction step scale $H_1$ by 1/2 and place four copies into the square quadrants. Rotate the curve in the first quadrant clockwise and the curve in the second quadrant counterclockwise, then connect the start and end points of these four curves using three line segments of size 1/2. The resulting curve is the 2nd order Hilbert curve $H_2$, as shown in Fig. 5d. Repeat the same procedure and the 3rd order Hilbert curve $H_3$ is constructed as shown in Fig. 5e.

## 3. Hilbert curve fractal current collectors (HFCC) and experimental setup

To emulate the planar type PCB–DMFC via a single cell structure, a test fixture was designed and constructed as shown in Fig. 6. The test fixture components include the anode flow board, gasket, anode current collector, gasket, MEA, gasket, cathode current collector, gasket and cathode airflow board. The anode and cathode flow boards are made of acrylic and both the anode and cathode current collectors are made of stainless steel 316L (SS316L). As this study focused on the current collector geometric effects on the DMFC performance, both the anode and cathode flow boards adopted SSFF which is almost the simplest flow field but has the capability to transport anode fuel or cathode air and remove the bubbles generated at the anode or water produced at the cathode air pretty well [9]. In this research, the anode and cathode flow boards are the same and the detailed dimensions are shown in Fig. 7a and the 3D solid drawing is shown in Fig. 7b. The width of the flow channel, the width of the rib and the depth of the flow channel are all 2 mm. The flow channel coverage percentage at the flow board of the activation zone is 50% at both the anode and cathode. A gasket is placed between two components to prevent leakage. The membrane electrode assembly (MEA) was sandwiched between the SS316L plates and used Nafion® 117 as the electrolyte with 4 mg $cm^{-2}$ catalyst Pt-Ru catalytic loaded onto the anode and 4 mg $cm^{-2}$ Pt loaded onto the cathode. The active single cell size in the experimental DMFC was 35 mm × 35 mm. The complete single DMFC test fixture assembly is shown in Fig. 8.

Performance measurements and DMFC comparisons with the 1st, 2nd, and 3rd Hilbert curve current collectors and a stan-

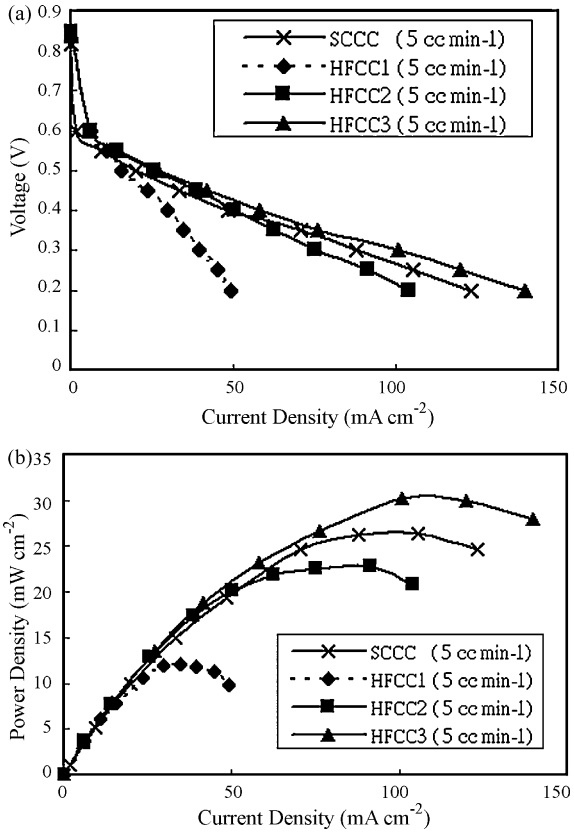


**Fig. 18.** Performance comparison of the DMFC with different current collectors under 5 cc min$^{-1}$ anode flow rate: (a) *I–V* curves, (b) *I–P* curves.

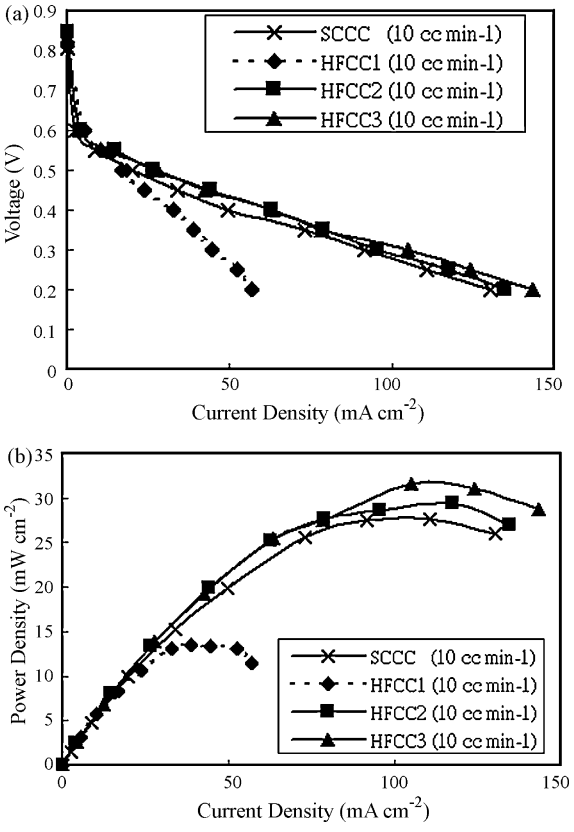


**Fig. 19.** Performance comparison of the DMFC with different current collectors under 10 cc min$^{-1}$ anode flow rate: (a) *I–V* curves, (b) *I–P* curves.

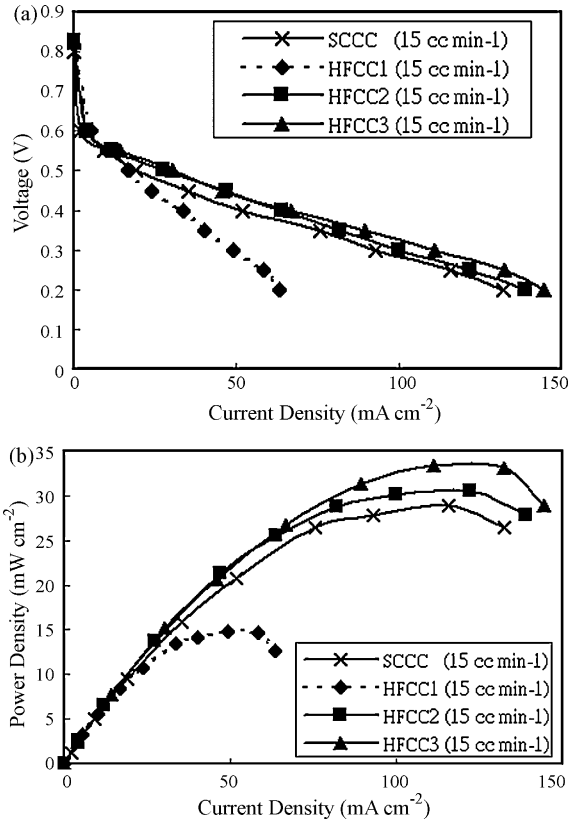


**Fig. 20.** Performance comparison of the DMFC with different current collectors under 15 cc min$^{-1}$ anode flow rate: (a) *I–V* curves, (b) *I–P* curves.

dard circle holes arrangement were conducted. To simplify the experiments and ensure cell stability, a DMFC with SS316L current collectors was used because SS316L has the advantages of easy machining, lower cost and good mechanical properties [26,27]. The reactive area of the MEA is 35 mm × 35 mm.The detailed dimensions are illustrated as follows. The size of each current collector is 95 mm × 95 mm × 2 mm.

Fig. 9 shows the standard circular hole current collector (SCCC), including the dimension and picture. Fig. 10 shows the 1st Hilbert curve fractal current collector (HFCC1), Fig. 11 shows the 2nd Hilbert curve fractal current collector (HFCC2) and Fig. 12 shows the 3rd Hilbert curve fractal current collector (HFCC3).

The geometric information on the current collectors is shown in Table 1. The width of the Hilbert curve for HFCC1, HFCC2, and HFCC3 were 2.2 mm, 2.2 mm, and 1.1 mm, respectively. The total perimeter length of opening in the current collector with SCCC, HFCC1, HFCC2, and HFCC3 openings were 614.12 mm, 266.90 mm, 555.65 mm, and 1117.82 mm, respectively. The total free open area in the current collectors with the SCCC, HFCC1, HFCC2, and HFCC3 openings were 612.5 mm$^2$, 288.75 mm$^2$, 606.37 mm$^2$, and 613.59 mm$^2$, respectively. The total free open ratio in the current collector with the SCCC, HFCC1, HFCC2, and HFCC3 openings were 50.00%, 23.50%, 49.40%, and 50.00%, respectively.

Fig. 13 is a schematic illustration of the experimental setup used in this research. The DMFC was placed into an environmental chamber with a methanol solution tank was placed in a temperature controlled water bath. The methanol solution was preheated and pumped into the DMFC using a squirm liquid pump. The airflow was driven using an air pump into the DMFC cathode. The airflow rate was controlled using an airflow regulator. A DC electric loader

was used to make the DMFC load. A data acquisition (DAQ) system was adopted to record the experimental data.

## 4. Results and discussion

The environmental conditions in all experiments were kept at 55 °C temperature and 60% RH. The anode was supplied with a 2 M MeOH/DI water solution methanol at flow rates of 5 cc $min^{-1}$, 10 cc $min^{-1}$, and 15 cc $min^{-1}$. The cathode side was fed air at a flow rate of 1000 cc $min^{-1}$.

### 4.1. Same geometry configuration under different anode flow rate

Both the anode and cathode current collectors adopted the same geometric configuration. Fig. 14 shows the performance comparison of the DMFC with standard circular hole current collectors (SCCC) at both the anode and cathode under different anode flow rates. The results show that the performances are close under different anode flow rates. The cell under 15 cc $min^{-1}$ anode flow rate showed the best performance, 10 cc $min^{-1}$ showed second and 5 cc $min^{-1}$showed the worst especially at the high current density range. Fig. 15 shows the performance comparison of the DMFC with HFCC1 at both the anode and cathode under different anode flow rate. The results show that the cell under 15 cc $min^{-1}$ anode flow rate presented the best performance, 10 cc $min^{-1}$ present second and 5 cc $min^{-1}$present the worst. This geometry does not have a uniform opening distribution in the current collector and a higher anode flow rate could provide fresh fuel instantly and drain the $CO_2$ bubbles smoothly. Fig. 16 is the performance comparison of DMFC with HFCC2 at both the anode and cathode under different anode flow rates. The results show that the cell under 5 cc $min^{-1}$ anode flow rate presented lower performance than 10 cc $min^{-1}$ and 15 cc $min^{-1}$. The cell performance under 15 cc $min^{-1}$ anode flow rate was higher than that for 10 cc $min^{-1}$. The HFCC2 opening distribution is more uniform than HFCC1 and could reduce the anode flow rate effect. Fig. 17 is the performance comparison of DMFC with HFCC3 at both the anode and cathode under different anode flow rates. The results show that the cell performances are close to each other under different anode flow rates. The cell performance under 15 cc $min^{-1}$ anode flow rate is the highest, 10 cc $min^{-1}$ the second and 5 cc $min^{-1}$ the worst.

Based on the above results the anode fuel flow rate could affect the cell performance significantly in the DMFC with HFCC1, which has the lowest total free open ratio and shortest total opening perimeter. The cell performance becomes higher with increasing anode flow rate, producing higher cell performance. For the DMFC with HFCC2, the cell performance increased significantly when the anode fuel flow rate increased from 5 cc $min^{-1}$ to 10 cc $min^{-1}$. Further increase in anode fuel flow rate from 10 cc $min^{-1}$ to 15 cc $min^{-1}$ increased the cell performance only slightly. The anode flow rate did not affect the cell performance obviously in the DMFC with SCCC. Compared the geometry of HFCC2 and SCCC, they have close total free open ratio (about 50%) but the SCCC has longer total perimeter length of openings than HFCC2. HFCC3 also has about 50% free open ratio but longer total opening perimeter length, which is about 1.9 times the SCCC. The anode flow rate does not affect the cell performance much. Therefore, enough fuel distribution area, i.e., the total free open ratio, would help the fuel be distributed to the MEA and produce $CO_2$ bubble drainage. A sufficient total opening perimeter length would provide more side to collect electrons from the current collector. Therefore, the anode fuel flow distribution and bubbles interference effects might be improved by increasing the anode flow rate. From the design viewpoint the planar type DMFC with a current collector with sufficient total free open ratio and total opening perimeter length is recommended.

### 4.2. Same anode flow with different geometric configuration of current collectors

This section discusses the DMFC performance with different geometric current collector configurations under the same anode flow rate. Fig. 18 is the performance comparison of the DMFC under 5 cc $min^{-1}$ anode flow rate. The results show that the DMFC with HFCC3 has the best cell performance, SCCC the second, HFCC2 the third, and HFCC1 worst. Fig. 19 is the performance comparison of the DMFC under 10 cc $min^{-1}$ anode flow rate. The results show that the DMFC with HFCC3 has the best cell performance, HFCC2 the second, SCCC the third, and HFCC1 worst. Fig. 20 is the performance comparison of the DMFC under 15 cc $min^{-1}$ anode flow rate. The results show the same trend as 10 cc $min^{-1}$ anode flow rate, the DMFC with HFCC3 has the best cell performance, HFCC2 the second, SCCC the third, and HFCC1 worst.

The lower total free open ratio and shorter total opening perimeter length in the current collectors lead to lower cell performance. Under the same total free open ratio, increasing the total opening perimeter length in the current collectors would significantly increase the cell performance.

## 5. Conclusions

This paper presented a DMFC with Hilbert curve fractal current collectors. The DMFC with the 3rd order Hilbert curve fractal current collectors showed the highest cell performance. The DMFC with the 1st order Hilbert fractal current collectors showed the lowest cell performance. Current collectors with more uniform opening distribution and higher total opening perimeter length could reduce the anode flow rate effect in the cell performance. In addition, the higher total free open ratio and total opening perimeter length in the current collectors could increase cell performance. The results from this study could be a useful reference for the future current collector design for the planar type DMFCs.

## Acknowledgement

The authors would like to acknowledge the financial supports from National Science Council of Taiwan, R.O.C. (NSC94-2212-E-149-004).

## References

[1] R. O'Hayre, S.-W. Cha, W. Colella, F.B. Prinz, Fuel Cell Fundamentals, John Wiley & Sons Ltd., 2006.
[2] J. Larminie, A. Dicks, Fuel Cell Systems Explained, 2nd ed., John Wiley & Sons Ltd., 2003.
[3] G. Apanel, E. Johnson, Fuel Cells Bull. (2004) 12.
[4] Fuel Cell Handbook, 5th ed., E&G Services, Parson Inc., Science Applications International Corporation, 2000.
[5] F. Barbir, PEM Fuel Cells, Elsevier Inc., 2005.
[6] T. Schultz, S. Zhou, K. Sundmacher, Chem. Eng. Technol. 24 (No. 12) (2001) 1223.
[7] H. Tsuchiya, O. Kobayashi, Int. J. Hydrogen Energy 29 (2004) 985–990.
[8] A. Hermann, T. Chaudhuri, P. Spagnol, Int. J. Hydrogen Energy 39 (2005) 1297–1302.
[9] H. Yang, T.S. Zhao, Electrochim. Acta 50 (2005) 3243–3252.
[10] R. O'Hayre, D. Braithwaite, W. Hermann, S.-J. Lee, T. Fabian, S.-W. Cha, Y. Saito, F.B. Prinz, J. Power Sources 124 (2003) 459–472.
[11] A. Schmitz, M. Traintz, S. Wagner, R. Hahn, C. Hebling, J. Power Sources 118 (2003) 162–171.
[12] A. Schmitz, S. Wagner, R. Hahn, H. Uzun, C. Hebling, J. Power Sources 127 (2004) 197–205.
[13] Y.-D. Kuan, S.-M. Lee, J.-Yi. Chang, M.-F. Sung, Proceedings of FuelCell2008 Sixth International Fuel Cell Science, Engineering and Technology Conference, Denver, Colorado, USA, June16–18, 2008, 2008.

[14] J.J. Huang, S.D. Wu, L.K. Lai, C.K. Chen, D.Y. Lai, J. Power Sources 161 (2006) 240–249.
[15] J.-Y. Chang, Y.-D. Kuan, S.-M. Lee, S.-R. Lee, J. Power Sources 184 (2008) 180–190.
[16] B.B. Mandelbrot, The Fractal Geometry of Nature, W.F. Freeman, San Francisco, 1982.
[17] D. Lee, W. Lin, J. AICHE 41 (1995) 2314–2317.
[18] G. Ledezma, A. Bejan, M. Errera, J. Appl. Phys. 82 (1997) 89.
[19] D. Pence, Micro-scale Thermophys. Eng. 6 (2002) 319–330.
[20] S. Lee, Y. Wang, C. Chen, J. Chin. Soc. Mech. Eng. 25 (2004) 547–556.
[21] C. Chen, Y. Juang, W. Lin, J. Mater. Process. Technol. 127 (2002) 146–150.
[22] K. Tuber, A. Oedegaard, M. Hermann, C. Hebling, J. Power Sources 131 (2004) 175–181.
[23] R. Crownover, Introduction to Fractals and Chaos, Jones and Bartlett Publishers, 1995.
[24] H. Peitgen, H. Jurgens, D. Saupe, Chaos and Fractals New Frontiers of Science, Springer-Verlag, 1992.
[25] D. Hilbert:, Mathematische Annale 38 (1891) 459–460.
[26] R. Makkus, A. Jansseen, F. de Bruijn, R. Mallant, Fuel Cells Bull. 17 (2000) 5–9.
[27] J. Wind, R. Späh, W. Kaiser, G. Böhm, J. Power Sources 105 (2002) 256–260.